

OPTIMIZATION OF SEALING PARAMETERS OF DOUBLE-SEALING PIPELINE REPAIR CLAMP¹

BINGJIE ZHAO

*Tianjin Key Laboratory for Advanced Mechatronic System Design and Intelligent Control, School of Mechanical Engineering, Tianjin University of Technology, Tianjin, China; and
National Demonstration Center for Experimental Mechanical and Electrical Engineering Education, Tianjin University of Technology, Tianjin, China
e-mail: zhaobjie@126.com*

SHULI ZHANG

CNOOC Safety Technology Services Co., Ltd, Tianjin, China

QIJUN GAO

*Tianjin Key Laboratory for Advanced Mechatronic System Design and Intelligent Control, School of Mechanical Engineering, Tianjin University of Technology, Tianjin, China; and
National Demonstration Center for Experimental Mechanical and Electrical Engineering Education, Tianjin University of Technology, Tianjin, China*

CANLIANG MIAO, TONGYU WANG

CNOOC Safety Technology Services Co., Ltd, Tianjin, China

Considering the key equipment of the pipeline clamp repair technology, this paper analyzes design of the pipeline repair clamp. Based on the damaged pipeline repair requirements, the design of a double-sealing pipeline repair clamp is established. The subsea pipeline in the Bohai Bay is considered as an example to develop a finite element model of a double sealing structure and calculate the sealing capacity, targeting a sealing pressure of 6 MPa. The parameters affecting the sealing capacity are studied. For circumferential sealing, the effects of distance between the rubber and the pipeline, distance between the ring and the pipeline, and the contact friction coefficient on the sealing capacity are analyzed. The design parameters of circumferential sealing are optimized by an orthogonal experimental design method. Further, the effect of the friction coefficient on the axial sealing capacity is studied, and design suggestions are put forward based on the analysis. The results of this study can provide guidance for the design and application of subsea pipeline repair clamps.

Keywords: seal, rubber, pressure, the orthogonal experimental design

1. Introduction

The clamp repair technology is used to repair an urban water supply pipeline, land oil and gas pipeline, subsea oil and gas pipeline, and chemical medium pipeline in chemical plants (Armando and Ray, 2011). It is mainly applied to repair leakage caused by local mechanical damage of the pipeline, corrosion perforation leakage, and crack leakage and thinning of pipe walls (DNV, 2007). According to the present project requirements, the clamp can either be connected to the damaged pipeline by welding or be installed on the part of the pipeline bolt fastening. The clamp repair technology has a low overall cost and a wide range of application.

¹Paper presented at the 5th International Conference on Material Strength and Applied Mechanics, MSAM 2022, Qingdao, Shandong, China

In the recommended practice, the sealing principle and enhancement principle of subsea pipeline repair clamps have been determined, and various sealing methods have been introduced for the clamp sealing. For the repair of pipeline defects, a metal sleeve has been studied, and the wall thickness of the metal sleeve has been optimized by the finite element method (Arif *et al.*, 2012). The grouted sleeve has been designed and its effect on pipeline integrity has been studied by the finite element method (Sum and Leong, 2014). A composite clamp with light weight and good corrosion resistance has been developed. The calculation method of the wall thickness of the composite clamp has been introduced, and the mechanical behavior of the composite clamp has been calculated by the finite element method (Sum *et al.*, 2016). A fiber-reinforced polymer composite clamp has been developed, and its design method has been described in detail and verified by experiments (Djukic *et al.*, 2015). For repair of pipelines with glass fiber-reinforced composite clamps, the reinforcement ability of the composite to the pipeline has been analyzed by the finite element method, and the minimum number of layers of the composite sleeve has been determined (Mazurkiewicz *et al.*, 2018). A finite element modeling has been performed for repair of pipelines using type B split sleeve (Crapps *et al.*, 2018).

The packer rubber with two different materials has been optimized numerically by Abaqus and validated by experiments (Zhao *et al.*, 2015a). The parameters affecting the sealing performance of the packer rubber have been analyzed (Zhao *et al.*, 2015b). Four factors have been identified as affecting the sealing performance of the packer rubber (Lan *et al.*, 2019). An enhanced subsea pipeline repair clamp has been designed by using rubber materials with different hardness (Zhang *et al.*, 2018), and the sealing structure of the clamp has been optimized (Zhang *et al.*, 2019). However, until now, the effects of the sealing parameters of double sealing clamps have not been systematically studied.

In this study, a double-sealing repair clamp is designed. According to the designed sealing structure and aiming at a sealing capacity of 6 MPa, a finite element model is established and the finite element simulation calculation is completed. The parameters affecting the circumferential sealing capacity of the clamp are studied. According to the influencing parameters, the clamp sealing parameters are optimized by an orthogonal experimental design. Further, the influencing parameters of the clamp axial seal are studied.

2. Design of pipeline repair clamp

Figures 1 and 2 show different views of the structure of the designed pipeline repair clamp based on the pipeline leakage repair requirements. The circumferential sealing rubber is compressed by a flange to realize circumferential sealing of the pipeline repair clamp. The two clamp bodies are tightened by master bolts, and then the axial sealing rubber is compressed to realize axial sealing of the clamp. During pipeline repair, the clamp should be installed at the damaged portion of the pipeline. The leaking part of the pipeline is sealed in the cavity of the clamp such that the leaking pipeline is isolated from the external environment and the leaking of the medium in the pipeline to the external environment is prevented, thus repairing the leaking pipeline.

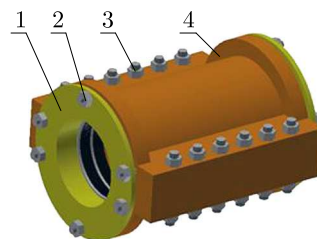


Fig. 1. Structure of the clamp (1): 1 – flange, 2 – flange bolts, 3 – master bolts, 4 – clamp body

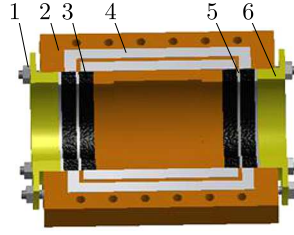


Fig. 2. Structure of the clamp (2): 1 – flange bolts, 2 – clamp body, 3 – circumferential sealing rubber, 4 – axial sealing rubber, 5 – clamp body, 6 – flange

3. Sealing performance of the pipeline repair clamp

By analyzing various parameters affecting the sealing capacity of the pipeline repair clamp, the ideal sealing design parameters can be obtained, allowing the pipeline repair clamp to meet sealing requirements and further guiding the design of the pipeline repair clamp.

The sealing material of the pipeline repair clamp is made of nitrile butadiene rubber (NBR), which is a hyperelastic material. Poisson’s ratio of NBR is approximately 0.5, which can be regarded as an incompressible material in finite element simulation. It has highly nonlinear characteristics. For the finite element simulation of rubber materials, the Mooney-Rivlin constitutive model is used as it describes mechanical behavior of rubber materials effectively, with not only a high fitting degree but also high calculation accuracy (Mooney, 1940; Xu *et al.*, 2021; Ramezani *et al.*, 2019).

The strain energy function is usually used to express physical properties of hyperelastic materials

$$I_1 = \lambda_1^2 + \lambda_2^2 + \lambda_3^2 \quad I_2 = \lambda_1^2\lambda_2^2 + \lambda_2^2\lambda_3^2 + \lambda_1^2\lambda_3^2 \quad I_3 = \lambda_1^2\lambda_2^2\lambda_3^2 \quad (3.1)$$

The rubber material is incompressible, then

$$I_3 = \lambda_1^2\lambda_2^2\lambda_3^2 = 1 \quad (3.2)$$

The strain energy function is expressed as

$$W = \sum_{i,j=0}^n C_{ij}(I_1 - 3)^i(I_2 - 3)^j \quad (3.3)$$

Considering the calculation cost and analysis accuracy, the second-order Mooney-Rivlin model is proposed for modeling and calculation

$$W = C_{10}(I_1 - 3) + C_{01}(I_2 - 3) \quad (3.4)$$

where C_{01} and C_{10} are material constants, W is strain density, I_1 and I_2 are the first and second strain invariants, and $\lambda_1, \lambda_2, \lambda_3$ are principal elongation ratios.

In the finite element modeling and calculation, the materials of the pipeline, clamp body, ring and flange are steel. The contact friction coefficient between parts is considered. The friction coefficient between rigid materials is set to 0.1, and that between the NBR sealing material and steel is preliminarily set to 0.3. The parameter properties of the two types of materials are shown in Table 1. Abaqus software is used to perform the finite element modeling and calculation. In the finite element mesh generation, the cell is divided by size control. For grid division, 4-node CAX4RH is used for rubber materials and CAX4R for steel materials.

Table 1. Material parameters of steel and rubber

Name	IRHD	Elastic modulus [MPa]	Poisson's ratio	C_{10}	C_{01}	G [MPa]	Density [kg/m ³]
Rubber	65	5.52	0.499	0.736	0.184	1.84	
Steel		210	0.3				7850

In the clamp repair technology, sealing is realized by the contact pressure between the rubber and the pipe outer wall and that between the rubber and the clamp body. By compressing the rubber, the maximum contact pressure on the above-mentioned contact surfaces is greater than or equal to the transmission medium pressure in the pipeline, thus repairing the damaged pipeline. Therefore, the maximum contact pressure can be used to judge the basis for sealing, as shown below

$$P_{max} \geq P \quad (3.5)$$

where P_{max} is the maximum contact pressure on the sealing surface [MPa], and P is the transmission medium pressure in the pipeline [MPa].

In the sealing pressure test using the liquid, the relationship between the maximum contact pressure and the transmission medium pressure in the pipeline is given as follows

$$P_{max} \geq 1.25P \quad (3.6)$$

In order to improve the reliability of contact surface sealing, the contact pressure on the contact surface between the rubber and the pipe outer wall and that between the rubber and the clamp body are calculated by finite element simulation by considering the maximum effective contact pressure (MECP) and average effective contact pressure (AECP). The MECP is defined as the maximum of the normal extreme values that can truly reflect the contact pressure. The AECP is derived from the arithmetic mean filtering method in an automatic control system. Arithmetic mean filtering finds $P(n)$ to minimize the sum of squares of the error between the value and each sampling value. The average effective contact pressure is defined as follows. In the calculation of this statistical method, the abnormal extreme value affecting the arithmetic mean is removed, and here it is the value that interferes with the authenticity of the contact force. The AECP is determined by the method of the arithmetic average. In finite element simulation, after removing the interference value, m samples are taken for the contact pressure P on the contact surface, and the arithmetic average value from the sum of the contact pressure values of m samples is obtained as the AECP value $\bar{P}(k)$

$$\bar{P}(k) = \frac{1}{m} \sum_{i=1}^m P_i \quad (3.7)$$

Then, for effective sealing, the AECP shall be greater than or equal to the transmission medium pressure in the pipeline

$$\bar{P}(k) \geq P \quad (3.8)$$

In the sealing pressure test using the liquid, the relationship between the AECP and the transmission medium pressure in the pipeline is as follows

$$\bar{P}(k) \geq 1.25P \quad (3.9)$$

3.1. Circumferential seal calculation

3.1.1. Finite element modeling

We consider an example of the maintenance of a 323 mm diameter oil and gas transmission pipeline widely used in the Bohai Bay. The outer diameter of the pipeline used for simulation is 323 mm, and the sealing structure is shown in Fig. 3. Other parameters used for the simulation model are shown in Table 2. r_n is inner radius of the ring, H_1 is height of the ring, r_p is outer radius of the pipe, R_1 is inner radius of the rubber, R_2 is outer radius of the rubber and the ring, H_2 is height of the rubber, r_c is inner radius of the clamp, and R_3 is outer radius of the clamp.

Table 2. Clamp computational model structure geometry parameters

Pipe		Ring		Clamp		Rubber	
r_p	161.5	r_n	161.5	r_c	161.5	R_1	165
		R_2	215	R_3	235	R_2	215
		H_1	10			H_2	50

All units are in mm

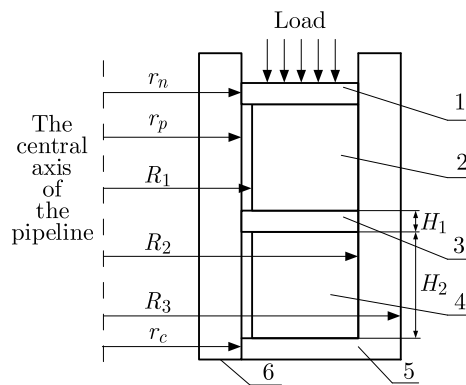


Fig. 3. Double seal structure: 1 – ring 1, 2 – rubber 1, 3 – ring 2, 4 – rubber 2, 5 – clamp, 6 – pipeline

A pre-load axial load is applied in the simulation, as shown in Fig. 3. A two-dimensional axisymmetric model is adopted. Under the axial load, the ring moves only in the axial direction of the pipe, limited by the inner wall of the clamp in the radial direction, and compresses the sealing ring. The rubber is allowed to move in the axial and radial directions of the pipe, while the pipe and clamp are presented from moving in all directions.

3.1.2. Result of FEA calculation

Mesh generation adopts size control. The clamp body, pipe, ring and rubber are meshed. Grid independence verification is performed by using six groups of data. Table 3 shows the finite element calculation results considering the contact pressure on the contact surface between rubber 1 and the outer wall of the pipe as the investigation object. The analysis results show that the maximum difference of the MECP is 0.06 MPa, which is considerably smaller than the maximum effective contact pressure, and the maximum difference of AECP is 0.09 MPa, which is considerably smaller than that of the average effective contact pressure. The results indicate that meshing has little effect on the calculation results. Finally, the grid division size of the clamp body, pipe and ring is 6 mm, and the grid division size of the rubber is 4 mm.

Table 3. Grid independence analysis

Serial number	Size of clamp, pipeline, and ring [mm]	Size of rubber [mm]	MECP [MPa]	AECP [MPa]
1	6	3	4.12	3.92
2	8	3	4.18	3.98
3	6	4	4.12	3.94
4	8	4	4.16	4.00
5	8	5	4.14	3.90
6	10	5	4.13	3.91

The circumferential sealing performance of the clamp is studied by the finite element method under the condition that the circumferential sealing pressure of the clamp meets 6 MPa. The applied axial load is 607.18 kN. The contact pressure nephogram is shown in Fig. 4, the contact pressure curve of each sealing surface is shown in Fig. 5, and the finite element calculation results of the contact pressure on the sealing surface are shown in Table 4.

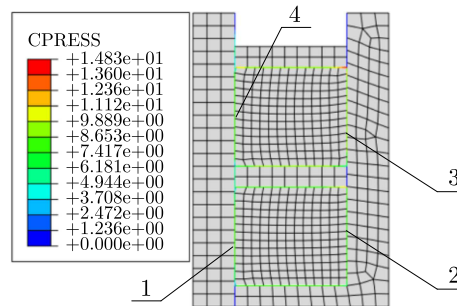


Fig. 4. Sealing surface contact pressure nephogram: 1 – surface 1, 2 – surface 2, 3 – surface 3, 4 – surface 4

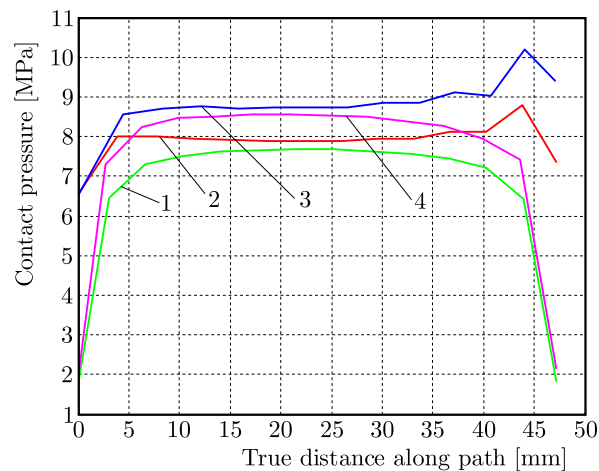


Fig. 5. Surface contact pressure curves

Table 4. Contact pressure of the sealing surface

Load [kN]	Sealing surface	AECP [MPa]	MECP [MPa]
607.18	1	7.53	7.68
	2	7.97	8.13
	3	8.80	9.12
	4	8.39	8.56

The sealing condition is that the contact pressure on the contact surface is greater than or equal to the sealing pressure. The AECP calculated by simulation shall meet a sealing pressure greater than or equal to 6 MPa and a test pressure greater than or equal to 7.5 MPa. The calculation results indicate that the AECP and MECP of the four sealing surfaces are greater than 7.5 MPa, meeting the sealing requirement that the test pressure is 1.25 times the design pressure; therefore, a double sealing structure is formed.

Comprehensively considering the contact pressure on sealing surfaces 1, 2, 3, and 4, the AECP and MECP of sealing surface 1 are the smallest. Therefore, as long as sealing surface 1 meets the sealing requirements, other sealing surfaces can also meet the sealing requirements, and the double sealing design can be realized. Thus, only the contact pressure of sealing surface 1 can be considered in the finite element calculation. Taking sealing surface 1 in rubber 2 as the main research object, the effects of distance between the rubber and the pipe, distance between the ring and the pipe, and a change in the friction coefficient on the circumferential sealing capacity of the clamp are studied.

- (1) The effect of distance between the rubber and the pipe (DBRP in Tables 5 and 8) on the sealing performance of the clamp is studied. The friction coefficient between rigid materials is set to 0.1. The contact friction coefficient between the sealing material and steel material is set to 0.3, and distance between the rubber and the pipe is varied as 0 mm, 2 mm, 4 mm, and 6 mm. Figure 6 shows the contact pressure curve of sealing surface 1 when a constant axial load of 607.18 kN is applied to the clamp, and the circumferential thickness of the rubber ring remains unchanged for 50 mm. The calculation results of the contact pressure of sealing surface 1 are shown in Table 5.

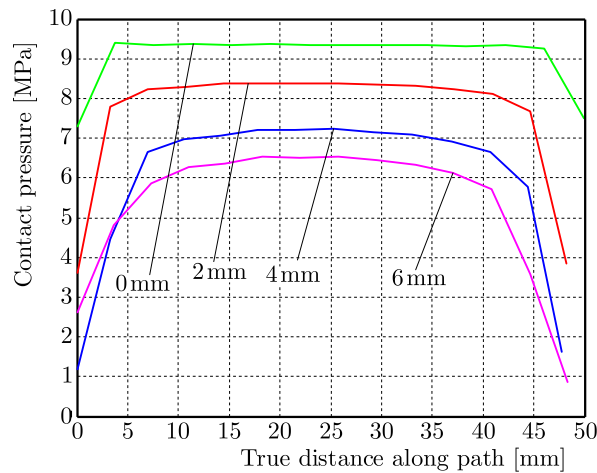


Fig. 6. Surface 1 contact pressure curves

Table 5. Contact pressure of the sealing surface 1

Load [kN]	DBRP [mm]	AECP [MPa]	MECP [MPa]
607.18	0	9.34	9.37
	2	8.30	8.39
	4	7.02	7.23
	6	6.26	6.53

The calculation results shown in Fig. 6 and Table 5 indicate that under the same axial load, with an increase in distance between the rubber and the pipe, the MECP and AECP on contact surface 1 gradually decrease. The increase of distance between the rubber and the pipe is not conducive to enhancing the sealing ability of the clamp; therefore, to

meet the repair requirements. The distance between the rubber and the pipeline can be appropriately reduced in the design.

- (2) The effect of distance between the ring and the pipe (DRP in Tables 6 and 8) on the sealing performance of the clamp is studied. The friction coefficient between rigid materials is set to 0.1, and the contact friction coefficient between the sealing material and steel is set to 0.3. The distance between the ring and the pipe is varied as 0 mm, 2 mm, 4 mm, and 6 mm. Figure 7 shows the contact pressure curve on sealing surface 1 under a constant axial load of 607.18 kN applied to the clamp. The calculation results of the contact pressure on sealing surface 1 are shown in Table 6.

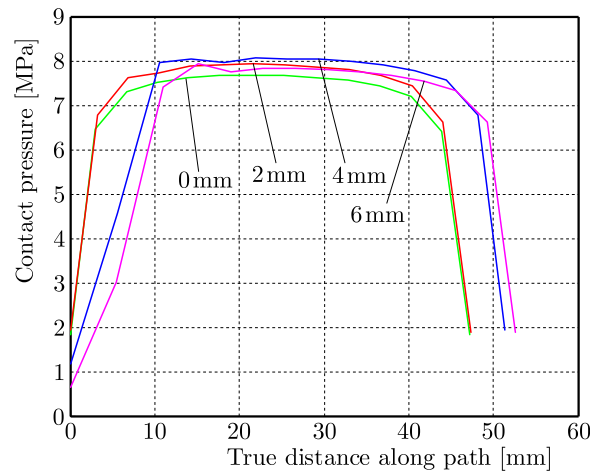


Fig. 7. Surface 1 contact pressure curves

Table 6. Contact pressure of the sealing surface 1

Load [kN]	DRP [mm]	AECP [MPa]	MECP [MPa]
607.18	0	7.53	7.68
	2	7.77	7.92
	4	7.93	8.06
	6	7.68	7.82

Figure 7 and Table 6 indicate that under the same axial load, when the distance changes from 0 to 4 mm, the MECP and the AECP on the contact surface gradually increase with a growth in distance between the ring and the pipe. These values are maximum when the distance is 4 mm. When the distance is 6 mm, both contact pressure values decrease.

- (3) The effect of the friction coefficient between the rubber and the rigid materials on the sealing performance of the clamp is studied. The friction coefficient between rigid materials is set to 0.1, while that between the rubber and the rigid materials is varied as 0.3, 0.4, 0.5, 0.6, and 0.7. Figure 8 shows the contact pressure curve of sealing surface 1 under a constant axial load of 607.18 kN applied to the clamp. The calculation results of the contact pressure on sealing surface 1 are shown in Table 7.

Figure 8 and Table 7 indicate that under the same axial load, with an increase of the contact friction coefficient, the MECP and AECP on surface 1 gradually decrease. The increase of the contact friction coefficient is not conducive to enhancing the sealing capacity of the clamp; therefore, it should be reduced appropriately in the design.

- (4) The parameters affecting the circumferential sealing performance of the clamp, mainly including distance between the rubber and the pipe, distance between the ring and the pipe, the contact friction coefficient between the rubber and the rigid materials, should

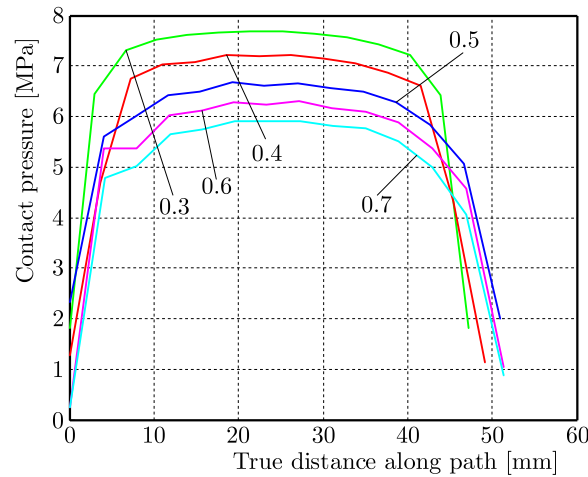


Fig. 8. Surface 1 contact pressure curves

Table 7. Contact pressure on sealing surface 1

Load [kN]	Friction coefficient	AECP [MPa]	MECP [MPa]
607.18	0.3	7.53	7.68
	0.4	7.02	7.21
	0.5	6.40	6.67
	0.6	5.98	6.30
	0.7	5.62	5.91

be optimized. To further study the combined effect of multiple parameters on the sealing performance and obtain more optimized parameters, an orthogonal experimental design method is proposed to study multiple parameters. The orthogonal experimental design is an efficient, fast and economic multi-factor experimental design method which can achieve results equivalent to those with a large number of comprehensive tests with the least number of tests (Wen *et al.*, 2022; Han *et al.*, 2021; Xu *et al.*, 2021; Dong *et al.*, 2022; Cheng *et al.*, 2022).

Considering the effect of a single factor on the sealing performance, among the three factors, distance between the rubber and the pipe is varied as 0 mm, 2 mm, and 4 mm; distance between the ring and the pipe is varied as 2 mm, 4 mm, and 6 mm, and the contact friction coefficient between the rubber and the rigid materials is varied as 0.3, 0.4, and 0.5. Table 8 shows the orthogonal experimental design parameters of the contact pressure on sealing surface 1 when a constant axial load of 607.18 kN is applied to the clamp, and the circumferential thickness of the rubber ring remains unchanged for 50 mm. The contact pressure curve on sealing surface 1 is shown in Fig. 9.

3.2. Axial seal calculation

Here, the axial sealing of the clamp is studied considering a clamp length of 1000 mm; the calculation model and geometric parameters of the axial double sealing structure are shown in Fig. 10. The two-dimensional axisymmetric model is adopted. During the finite element simulation, clamp body 1 can only move in the Y direction. The load is applied to clamp body 1 by bolts. Clamp body 2 is completely fixed. The friction coefficient between rigid materials is set to 0.1, and that between the sealing material and steel is set to 0.3.

Table 8. Orthogonal experimental design parameters

Serial number	DBRP [mm]	DRP [mm]	Friction coefficient	AECP [MPa]	MECP [MPa]
1	0	2	0.3	9.90	10.10
2	0	4	0.4	9.77	9.97
3	0	6	0.5	9.13	9.29
4	2	2	0.4	8.25	8.38
5	2	4	0.5	7.96	8.10
6	2	6	0.3	8.64	8.80
7	4	2	0.5	6.53	6.68
8	4	4	0.3	7.61	7.76
9	4	6	0.4	6.83	7.10

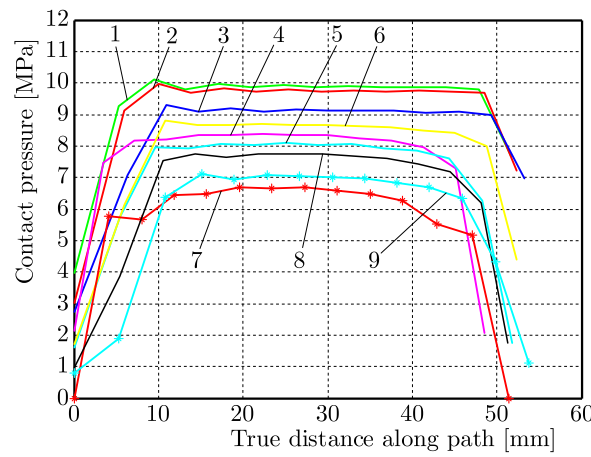


Fig. 9. Surface 1 contact pressure curves

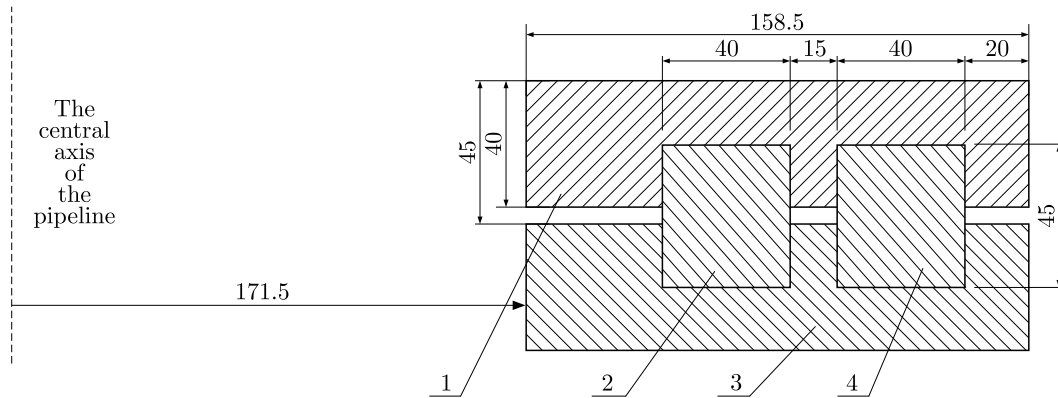


Fig. 10. Clamp computational model structure: 1 – clamp 1, 2 – rubber 1, 3 – clamp 2, 4 – rubber 2

The load applied by the bolt is 626.08 kN. The sealing surface contact pressure nephogram of the simulation calculation results is shown in Fig. 11, and the contact pressure curve of the sealing surface is shown in Fig. 12.

In rubber 1, sealing surfaces 1 and 2 are the main sealing surfaces. In rubber 2, sealing surfaces 3 and 4 are the main sealing surfaces. The contact pressure on the four sealing surfaces is the same. The AECP and the MECP on the contact surface are 7.52 MPa and 7.56 MPa, respectively. The sealing condition is that the contact pressure of the contact surface is greater

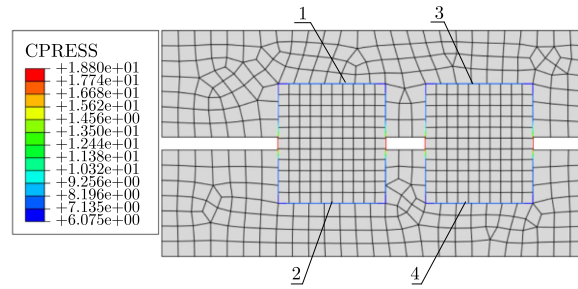


Fig. 11. Sealing surface contact pressure nephogram. 1 – surface 1, 2 – surface 2, 3 – surface 3, 4 – surface 4

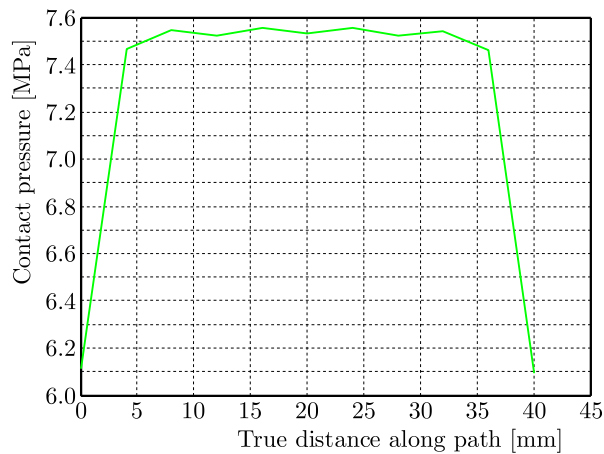


Fig. 12. Surface contact pressure curve

than or equal to the sealing pressure. The AECP calculated by simulation shall meet a sealing pressure greater than or equal to 6 MPa and a test pressure greater than or equal to 7.5 MPa. In the calculation results, the AECP and MECP of the four sealing surfaces are greater than 7.5 MPa, meeting the sealing requirements that the test pressure is 1.25 times the design pressure; thus, a double sealing structure is formed.

The effect of the contact friction coefficient on the sealing performance of the clamp is studied. In the simulation calculation, the contact friction coefficients between the rubber and the clamp body are set as 0.3, 0.4, 0.5, 0.6, and 0.7. Figure 13 shows the contact pressure curve on the sealing surface under a constant load of 626.08 kN applied to the clamp. The calculation results of the contact pressure of the sealing surface are shown in Table 9.

Table 9. Contact pressure on the sealing surface

Load [kN]	Friction coefficient	AECP [MPa]	MECP [MPa]
626.08	0.3	7.52	7.56
	0.4	7.52	7.56
	0.5	7.52	7.56
	0.6	7.52	7.56
	0.7	7.52	7.56

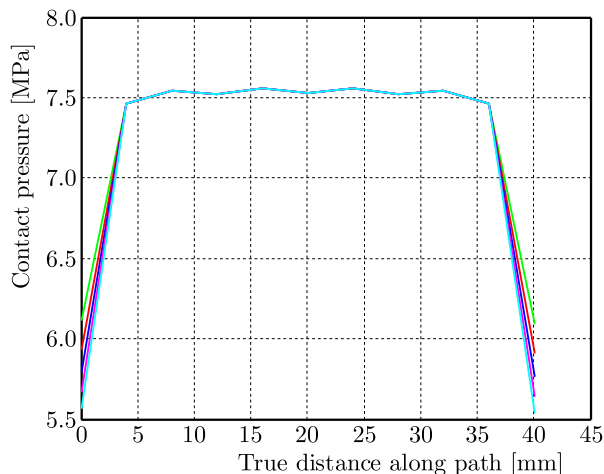


Fig. 13. Surface contact pressure curves

4. Results

The analysis of the circumferential sealing calculation results shown in Table 8 indicates that in 9 groups of simulation calculation, the AECF values are 6.53 MPa for group 7 and 6.83 MPa for group 9, both values being less than 7.5 MPa. The AECF values of the other 7 groups are greater than 7.5 MPa, with group 1 having the highest value of 9.90 MPa.

The analysis of the axial sealing calculation results shown in Fig. 13 and Table 9 indicates that under the same load, although the friction coefficients differ, the AECF and MECF of the contact surface are equal.

5. Discussions

For circumferential sealing, the AECF and MECF of group 1 are the largest and those of group 7 are the smallest (Table 8). The difference of the AECF between the two groups is 3.47 MPa. The design parameters of group 7 and 9 do not meet the test pressure requirements. When the same axial force is applied, the data of group 1 can be selected as optimal design parameters, which can maximize the sealing pressure of the clamp. Under a constant applied axial force, the AECF and MECF differ owing to the varying design parameters. Through the orthogonal experimental design, more ideal design parameters can be optimized and obtained.

For axial sealing, the contact friction coefficient has no effect on the seal contact pressure (Table 9). Therefore, in the design of the type of sealing considered in this study, the effect of the contact friction coefficient on the sealing performance can be ignored, which is conducive to the manufacturing of the sealing material and clamp body.

6. Conclusion

Considering the repair requirements of the Bohai Bay subsea pipeline, to improve the sealing performance of the clamp, a double-sealing structure design of the subsea oil and gas pipeline repair clamp was carried out. Aiming at a sealing capacity of 6 MPa, the sealing capacity of the double-sealing repair clamp was modeled and calculated by the finite element method. Taking the average effective contact pressure and the maximum effective contact pressure as the evaluation criteria, the sealing capacity of the repair clamp and the parameters affecting the sealing performance were studied.

- The parameters affecting circumferential sealing were studied, and their individual effect on sealing ability were determined. Three of the parameters were studied by the orthogonal experimental design and optimized.
- The contact friction coefficient was found to have no effect on the axial seal ability of the clamp; therefore, its effect can be ignored in the design of axial sealing. In the design of the clamp, the requirements of pipeline repair and repair clamp manufacturing technology should be comprehensively considered and, accordingly, the sealing design parameters should be selected appropriately.

References

1. ARIF A.F.M., AL-NASSAR Y.N., AL-QAHTANI, H., KHAN S.M.A., ANIS M., ELEICHE A.M., INAM M., AL-NASRI N.I., AL-MUSLIM H.M., 2012, Optimization of pipe repair sleeve design, *Journal of Pressure Vessel Technology*, **134**, 5, 051702-1-10
2. ARMANDO R., RAY A., 2011, Deep water pipeline emergencies, managing risk and cost, the coownership solution, *Proceedings of the 6th International Offshore Pipeline Forum*, Houston, Texas, **6003**, 1-4
3. CHENG Y.F., LUO X.Y., WANG P.F., YANG Z.H., HUANG J., GU J.X., ZHAO W.S., 2022, Multi-objective optimization of thermal-hydraulic performance in a microchannel heat sink with offset ribs using the fuzzy grey approach, *Applied Thermal Engineering*, **201**, 1-17
4. CRAPPS J.M., YUE X., BERLIN R.A., SUAREZ H.A., PRIBYTKOV P.A., VYVIAL B.A., PROEGLER J.S., 2018, Strain-based pipeline repair via type B sleeve, *International Journal of Offshore and Polar Engineering*, **28**, 3, 280-286
5. DJUKIC L.P., SUM W.S., LEONG K.H., HILLIER W.D., ECCLESHALL T.W., LEONG A.Y.L., 2015, Development of a fibre reinforced polymer composite clamp for metallic pipeline repairs, *Materials and Design*, **70**, 68-80
6. DNV, 2007, Recommended Practice DNV-RP-F113 Pipeline Subsea Repair (DNV-RP-F113-2007), Norway, Det Norske Veritas
7. DONG L., LI Y.B., HUANG M.H., HU X., QU Z.J., LU Y., 2022, Effect of anodizing surface morphology on the adhesion performance of 6061 aluminum alloy, *International Journal of Adhesion and Adhesives*, **113**, 1-9
8. HAN Z.Y., MA D., CHEN Q.Y., WANG Y.H., 2022, Orthogonal test design for optimization of synthesis of Bi₂WO₆ superstructure with high photocatalytic activity by hydrothermal method, *Journal of Chemical Technology and Biotechnology*, **97**, 943-949
9. LAN W.J., WANG H.X., ZHANG X., CHEN S.S., 2019, Sealing properties and structure optimization of packer rubber under high pressure and high temperature, *Petroleum Science*, **16**, 3, 632-644
10. MAZURKIEWICZ L., MALACHOWSKI J., DAMAZIAK K., TOMASZEWSKI M., 2018, Evaluation of the response of fibre reinforced composite repair of steel pipeline subjected to puncture from excavator tooth, *Composite Structures*, **202**, 1126-1135
11. MOONEY, M.J., 1940, A theory of large elastic deformation, *Journal of Applied Physics*, **11**, 9, 582-592
12. RAMEZANI M.A., YOUSEFI S., FOULADI N., 2019, An experimental and numerical investigation of the effect of geometric parameters on the flexible joint nonlinear behavior for thrust vector control, *Proceedings of the Institution of Mechanical Engineers, Part G: Journal of Aerospace Engineering*, **233**, 8, 2772-2782
13. SUM W.S., LEONG K.H., 2014, Numerical study of annular flaws/defects affecting the integrity of grouted composite sleeve repairs on pipelines, *Journal of Reinforced Plastics and Composites*, **33**, 6, 556-565

14. SUM W.S., LEONG K.H., DJUKIC L.P., NGUYEN T.K.T., LEONG A.Y.L., FALZON P.J., 2016, Design, testing and field deployment of a composite clamp for pipeline repairs, *Plastics, Rubber and Composites*, **45**, 2, 81-94
15. WEN Z.H., JIANG S.D., LUO C.Y., XIA X.F., LIANG Y.Y., ZHANG L.Y., 2022, Assessment of ablation damage on quartz ceramics through experiment and 3D modelling considering a dynamic heat source, *Ceramics International*, **48**, 3, 3515-3526
16. XU B., MA Q.Y., HUANG D.G., 2021, Research on energy harvesting properties of a diffuser-augmented flapping wing, *Renewable Energy*, **180**, 271-280
17. XU P., QU C.J., YAO S.G., YANG C.X., WANG A., 2021, Numerical optimization for the impact performance of a rubber ring buffer of a train coupler, *Machines*, **9**, 10, 1-20
18. ZHANG F.Y., JIANG X.M., WANG H.H., SONG N.N., CHEN J.L., DUAN J.Y., 2018, Mechanical analysis of sealing performance for compression packer rubber tube, *Mechanics and Industry*, **19**, 3, 1-10
19. ZHANG F.Y., SHUI H.C., ZHANG Y.F., 2019, Parameter optimization of sealing performance for packer rubber, *Industrial Lubrication and Tribology*, **71**, 5, 664-671
20. ZHAO B.J., ZHU H.W., ZHANG S.L., ZHANG J.Y., TANG D.Y., 2015a, Design of subsea oil and gas pipeline repair clamp, *Proceedings of the ASME 2015 Pressure Vessels and Piping Conference*, 1-5
21. ZHAO B.J., ZHU H.W., ZHANG S.L., ZHANG J.Y., TANG D.Y., 2015b, Research of sealing property to subsea oil and gas pipeline repair clamp, *Proceedings of the ASME 2015 Pressure Vessels and Piping Conference*, 1-6

Manuscript received March 22, 2022; accepted for print April 26, 2022